Computers & Industrial Engineering 149 (2020) 106812

Contents lists available at ScienceDirect

Computers & Industrial Engineering

journal homepage: www.elsevier.com/locate/caie

Stochastic optimization for flow-shop scheduling with on-site renewable energy generation using a case in the United States

Shasha Wang [a,*], Scott J. Mason [a], Harsha Gangammanavar [b]

[a] Department of Industrial Engineering, Clemson University, Clemson, SC, USA
[b] Department of Engineering Management, Information, and Systems, Southern Methodist University, Dallas, TX, USA

ARTICLE INFO

Keywords:
Production scheduling
Flow shop
Renewable energy
Stochastic programming
Multi-objective programming

ABSTRACT

On-site renewable energy provides great opportunities for manufacturing plants to reduce energy costs when faced with time-varying electricity prices. To efficiently utilize on-site renewable energy generation, production schedules and energy supply decisions need to be well investigated. In this paper, we present a two-stage, multi-objective stochastic program for flow shops with sequence-dependent setup. The first stage provides optimal schedules to minimize the total completion time. The second stage determines the energy supply decisions to minimize energy costs under a time-of-use electricity pricing scheme. The power demand of the production is met by on-site renewable generation, supply from the main grid, and energy storage system. An epsilon-constraint algorithm integrated with L-shaped method is proposed to analyze the problem. Sets of Pareto optimal solutions are provided for decision-makers. Our results show that the energy cost of setup operations is relatively high such that it cannot be ignored. Further, using solar or wind energy saves energy costs significantly. While, utilizing solar energy can reduce more.

1. Introduction

Today, protecting the environment is one of the most critical issues faced by citizens of the world. While, with the development of economic globalization, global demand for almost any type of product is continuously growing. As a result, the industrial sector has a high energy demand to satisfy production demand. For example, the industrial sector accounted for 32% of total U.S. energy consumption in 2018 (Energy Information Adiministration, 2020a) according to a report from the U.S. Energy Information Administration. The main energy sources used by the sector are natural gas, petroleum, electricity, renewable sources, and coal. Although the share of renewable sources has been increasing over the past 60 years, it is still less than 10% of all energy sources. As we know, non-renewable energy sources can cause environmental issues, especially the emission of greenhouse gas (GHG). Another U.S. Energy Information Administration report claims that the industrial sector consumes about 25% of all electricity in use (Energy Information Adiministration, 2020b). To meet excessive peak electricity demands and decrease GHG emissions, load shifting and utilizing renewable resources are under consideration by Governments, society, and industry. Load shifting, which is also known as demand response, allows to curtail or shift energy demands in response to economic incentives. In a smart grid, any kind of end-use customer can gain benefits from adopting a demand response program. While, industrial sector has the potential to take more advantage of cost reduction by utilizing demand response (Wang, Gangammanavar et al., 2019).

Time-of-use (TOU) electricity pricing schemes vary prices during the day. Higher (lower) costs are charged during peak (off-peak) demand hours. TOU pricing schemes are used by utilities to motivate manufacturing plants to reduce consumption at peak times by shifting energy use from peak hours to off-peak hours. This shifting activity, which is referred to as demand response, can increase time-related scheduling objectives. Energy-cost-aware (ECA) manufacturing is a way to utilize demand response. Its objective is to minimize energy costs at the operational level by determining optimal job scheduling and/or lot-sizing while considering time-varying electricity prices (Sharma et al., 2015). Using on-site electricity generators, some industrial facilities produce electricity for use. In an ECA manufacturing system, industrial facilities also can sell some of the electricity that they generate back to the power grid for compensation.

An effective way to reduce GHG emissions is to utilize environment-friendly renewable energy resources, which have received significant research attention in recent years. Renewable resources are the fastest growing among all energy resources, with their consumption expected to increase by an average 2.3% per year between 2015 and 2040, according to the U.S. Energy Information Administration (Energy Information Adiministration, 2017). Moreover, some governments and

* Corresponding author.
E-mail address: shashaw@g.clemson.edu (S. Wang).

https://doi.org/10.1016/j.cie.2020.106812
Received 13 April 2020; Received in revised form 18 August 2020; Accepted 1 September 2020
Available online 4 September 2020

Nomenclature

Sets

B	Set of ESSs; indexed by $i = 1, 2, \ldots \lvert B \rvert$
J	Set of jobs; indexed by $j = 1, 2, \ldots \lvert J \rvert$
F	Set of job families; indexed by $f, g = 1, 2, \ldots \lvert F \rvert$
M	Set of machines; $m = 1, 2, \ldots \lvert M \rvert$
R	Set of renewable generators; $r = 1, 2, \ldots \lvert R \rvert$
T	Set of time periods; $t = 1, 2, \ldots \lvert T \rvert$

Parameters

w_j	Weight (priority) of job j
l	Length of a time slot [h]
p_{mj}	Processing time of job j on machine m [h]
s_{fg}	Setup time between job family f and g [h]
b_i^{min}	Minimum charging/discharging rate of ESS i [kW]
b_i^{max}	Maximum charging/discharging rate of ESS i [kW]
E_i^{min}	Minimum energy level of ESS i [kWh]
E_i^{max}	Maximum energy level of ESS i [kWh]
q_{mj}^{y}	Unit power consumed by processing job j on machine m [kW]
q_{mf}^{z}	Unit power consumed by idling at family f on machine m [kW]
q_{mfg}^{l}	Unit power consumed by a setup between job family f and g on machine m [kW]
c_t^d	Unit energy purchasing cost in time period t [$/kWh]
c_t^u	Unit energy selling price in time period t [$/kWh]
c_{it}^E	Unit energy storage cost of ESS i in time period t [$/kWh]
ρ_t	= 1 if the manufacturing plant is allowed to feed power into the electricity grid during time period t when the selling price $c_t^u \leq$ purchasing price c_t^d, 0 otherwise
$\tilde{\omega}_{rt}$	Random variable, power generated by renewable generator r at time t [kW]

Decision Variables

x_{mjt}	= 1 if job j is started on machine m at the beginning of time period t; otherwise = 0
y_{mjt}	= 1 if job j is processed on machine m during time period t; otherwise = 0
z_{mft}	= 1 if machine m is idle at job family f during time period $[t, t+1)$; otherwise = 0
v_{mfgt}	= 1 if machine m starts to make a setup operation for changing job family f to job family g at the beginning of time period t; otherwise = 0
o_{mfgt}	= 1 if machine m is doing a setup for changing job family f to job family g during time period t; otherwise = 0
d_t	Power purchased from the grid in time period t [kW]
u_t	Power sold to the grid in time period t [kW]
b_{it}	ESS charging/discharging rate during time period t [kW]. When b_{it} is positive, the ESS i is in charging status; otherwise, it is in discharging status
E_{it}	Energy state of ESS i in time period t [kWh]
a_t	Underutilized renewable generation in time period t [kW]

Acronyms and Abbreviations

GHG	Greenhouse gas
TOU	Time-of-use
ECA	Energy-cost-aware
ESS	Energy storage system
MILP	Mixed-integer linear program
ESF	Extensive scenario formulation
TWCT	Total weighted completion time
EC	Energy cost
2-SP	Two-stage stochastic program
SAA	Sample average approximation
CI	Confidence interval

organizations such as RE100 have committed to encouraging businesses to consider using 100% renewable power. According to its website, UPS invested $18 million in on-site solar panels, which expanded UPS's solar power generating capacity by 10 megawatts in 2017. Further, it is estimated that on-site wind energy resource development is feasible for about 44% of the continental U.S.'s buildings, according to a report by the National Renewable Energy Laboratory (Eric et al., 2016).

Unfortunately, the availability of wind and solar energy, which are two significant renewable energy resources, is uncertain, as it fluctuates with weather variations. Generation can vary at different times over a day and at the same time period over different days. Properly addressing the uncertainties inherent in renewable energy resources can mitigate potential scheduling solution inaccuracies. Further, developing effective strategies for handling the intermittent nature of renewable energy resources can improve the effectiveness of renewable energy utilization in production environments. To mitigate renewable energy availability challenges, energy storage systems (ESSs) are utilized to store intermittent renewable energy and use it when needed.

To the best of our knowledge, Liu (2016) presents the first study that integrates renewable energy supply into production scheduling while considering the uncertainty of renewable energy availability using interval number theory. Unfortunately, little research has been done since that simultaneously considers both ECA production scheduling and the utilization of uncertain renewable resources for energy generation. Given this motivation, we study a flow shop scheduling problem with sequence-dependent setups under a TOU pricing scheme. Power purchased from the main grid, generated by grid-connected on-site renewable generators such as wind turbines and solar panels, and discharged from ESSs are available energy sources for the manufacturing process under study. Energy consumption is machine status-related, as job processing, production setups, and machine idling consume different amounts of energy.

Fig. 1 describes the methodological approaches used in this research. We first formulate a two-stage, bi-objective stochastic ECA problem. Then the problem is solved through a ϵ-constraint framework with L-shaped method. Finally, experiments were conducted to illustrate the performance of our proposed algorithm and its effectiveness in realizing energy-related objectives in manufacturing. The main contributions of this research are threefold: (1) we study an ECA problem that integrates an energy procurement problem with a flow shop scheduling problem to minimize total weighted completion time and energy costs simultaneously by determining optimal job schedules and energy supply decisions; (2) we develop a two-stage, multi-objective stochastic

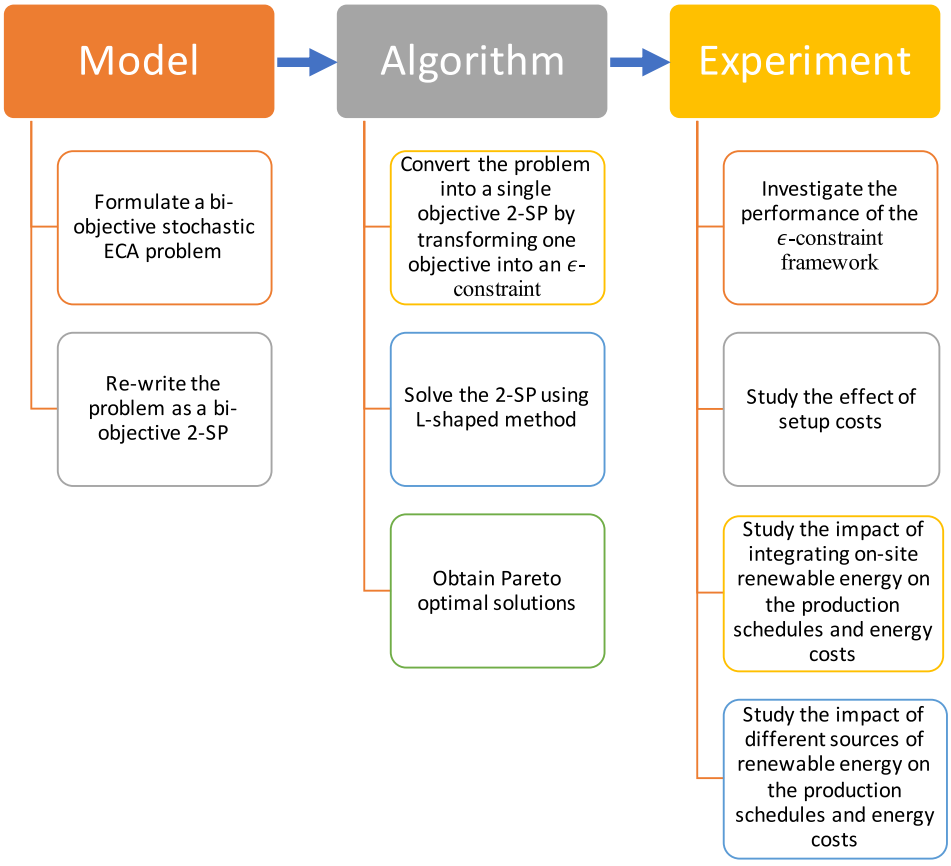

Fig. 1. Flow chart of methodological approaches performed in this research.

problem for the ECA problem. In the first stage, we propose a time-indexed, mixed-integer linear program (MILP) which captures several practical features of the flow shop scheduling problem. The second stage determines the energy transactions between the manufacturing plant and the power grid in the context of uncertain renewable energy and ESSs under a TOU pricing scheme; (3) we conduct a case study to investigate the performance of our algorithm, the effects of setups on energy cost, and demonstrate the potential benefits of utilizing on-site renewable resources and ESSs.

The rest of the paper is organized as follows. After the current literature is reviewed in Section 2, our mathematical model is presented in Section 3. Then, two-stage, multi-objective decomposition algorithms are implemented in Section 4, followed by a discussion of our computational experiments in Section 5. Finally, we offer conclusions and future research directions in Section 6.

2. Literature review

As many areas of the world are facing environmental issues surrounding the consumption of fossil fuels and concomitant GHG emissions, efforts to make production scheduling sustainable have become a key focus for many companies. Lots of literature on energy-aware production scheduling has evolved in recent years. Biel and Glock (2016), Gahm et al. (2016), and Giret et al. (2015) present a comprehensive review of this research stream. Giret et al. (2015) review the existing literature on sustainable scheduling and focus on environmental and economic development. Biel and Glock (2016) provide a survey on decision support models for energy-efficient production planning. Gahm et al. (2016) develop a framework for energy-efficient scheduling and classify the literature into three aspects–energetic coverage, energy supply, and energy demand. Gahm et al. (2016) state that machine processing states and job-related features both impact energy consumption during production operations, non-processing states such as machine idling, system on/off, and setups can also affect energy consumption requirements.

Yildirim and Mouzon (2012) propose a multi-objective framework for a single machine scheduling problem to minimize both energy consumption and job completion time by turning off the machine instead of leaving it idle when not in use. Liu et al. (2017) study a flow shop scheduling problem with state-dependent setup times to minimize energy consumption and tardiness penalties. After introducing fuzzy set theory to describe the uncertainty of processing time and due dates, an improved hybrid genetic algorithm is developed for solving the problem.

Luo et al. (2013) investigate a hybrid flow shop scheduling problem under a four-period TOU pricing scheme to minimize makespan and power consumption. Their experimental results show that increasing the length of each TOU period can reduce electricity costs without affecting makespan. Similarly, under a TOU tariff, Ding et al. (2016) propose a time-interval-based mixed-integer, linear model and a column generation heuristic for a parallel machine scheduling problem to minimize electricity costs while keeping the makespan within a given production deadline. Understanding the tradeoff between electricity costs and makespan can provide insights for management to help determine the maximum acceptable production time under TOU pricing schemes.

Moon and Park (2014) investigate production scheduling problems integrated with on-site renewable generation, fuel cells, and ESSs. They propose a model with two subproblems for a flexible job shop to minimize the sum of makespan-related production costs, the cost of purchasing power from the grid, the cost of distributed generations, and the cost of an ESS under a TOU pricing scheme. The first subproblem is a production scheduling problem with a given energy schedule, while the second subproblem is an energy scheduling problem for a given

Table 1
Summary of reviewed ECA production scheduling problems.

Study	Machine environment	Machine status	RES	Stochastic	ESS
Yildirim and Mouzon (2012)	Single machine	Processing, idling, and ON/OFF	–	–	–
Liu et al. (2017)	Flow shop	Processing, idling, state-dependent setup, and ON/OFF	–	–	–
Luo et al. (2013)	Hybrid flow shop	Processing and idling	–	–	–
Ding et al. (2016)	Parallel machine	Processing	–	–	–
Moon and Park (2014)	Flexible job shop	Processing and idling (no cost)	Yes	No	Yes
Zhai et al. (2017)	Flow shop	Processing, idling, and ON/OFF	Wind	No	–
Zhang et al. (2017)	Hybrid flow shop	Processing	Solar	No	Yes
Liu (2016)	Single machine	Processing	Yes	Yes	Yes
Biel et al. (2018)	Flow shop	Processing	Wind	Yes	–
Fazli Khalaf and Wang (2018)	Flow shop	Processing	Wind & Solar	Yes	Yes

flexible job shop. By solving these two subproblems alternately and repeatedly, a near-optimal solution is found. In their model, Moon and Park (2014) assume that the minimum and maximum amounts of renewable energy available for each time period within the planning horizon are known in advance. Then the amount of energy generated for a given time period is determined by the model. Zhai et al. (2017), who study a flow shop scheduling problem in the context of a real-time pricing scheme, also consider on-site renewable generation. Time series models are used to forecast hourly wind speeds and electricity prices, which increase data accuracy as compared to using the fixed intervals adopted by Moon and Park (2014). After obtaining forecast data, hourly wind speeds and electricity prices are fed into a manufacturing scheduling model to minimize energy costs. Unfortunately, this procedure requires that all data is predetermined without any consideration of uncertainty. Similarly, Zhang et al. (2017) investigate the effect of on-site photovoltaic and ESSs on a flow shop under a TOU pricing scheme. However, the uncertainty of solar generation is not considered in the study.

Liu (2016) presents a mathematical model for a single-machine scheduling problem integrated with renewable generation and an ESS. Liu (2016) represents the uncertainty of renewable energy resources by using interval number theory. The energy generated by renewable energy resources during each time period is bounded by an interval and the interval boundaries are randomly generated from a uniform distribution. The author assumes that the plant will purchase any power needed from the main grid if the renewable energy stored in batteries runs out in any time period. Two models are considered: (1) simultaneously minimizing total weighted flow time and GHG emissions using a lexicographic-weighted Tchebycheff method and (2) minimizing total weighted flow time by considering a GHG emission constraint.

Biel et al. (2018) propose a two-stage stochastic optimization procedure for a flow shop scheduling problem with on-site wind power under a TOU pricing scheme to minimize total weighted flow time and energy costs. In the first stage, a bi-objective MILP is used to evaluate a number of generated wind power scenarios which form an extensive scenario formulation (ESF). A weighted sum algorithm is used to tackle multiple objective functions. Then, based on real-time wind power data, energy supply decisions are adjusted in the second stage. Fazli Khalaf and Wang (2018) propose a two-stage stochastic MILP for a flow shop problem with on-site renewable resources and ESS under day-ahead and real-time electricity pricing schemes. The first stage determines job schedules and minimizes energy purchase cost procured from the day-ahead plan by considering forecasted renewable energy generation, while the second stage compensates for the mismatch between forecasted and actual renewable energy and minimizes energy costs under a real-time pricing scheme.

As Table 1 shown, only a few research studies have considered ECA production scheduling with stochastic renewable energy sources simultaneously. Further, sequence-dependent setups, which occur when production switches between different job families (Wang, Kurz et al., 2019), have been ignored in the literature. These setups not only affect time-related objectives but also affect energy costs and demand requirements (Allahverdi & Soroush, 2008). Motivated by these gaps in the literature, the main goal of our study is to examine these important topics.

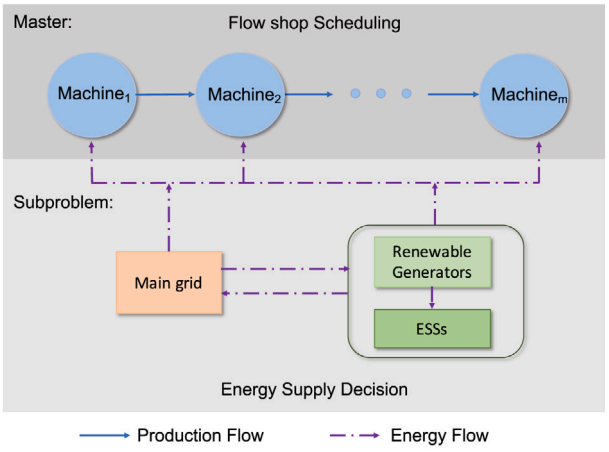

Fig. 2. A flow shop system with production and energy flow.

3. Problem formulation

Consider a flow shop comprised of $|M|$ production machines. A set of jobs J of varying weights (priorities) w_j is released at the beginning of the time horizon of interest. Each job $j \in J$ must be processed with processing time p_{mj} on each machine $m \in M$ sequentially. A sequence-dependent setup time is required for changeovers when the job family changes from $f \in F$ to $g \in F \setminus \{f\}$ on any machine. Different machine statuses (i.e., job processing, setup, and idling) consume different amounts of energy. The energy required for operating machines can be purchased from the main power grid, generated by on-site renewable generators, and/or discharged from ESSs. On-site renewable generation can be used to run production, charge ESSs, and/or be sold to the main grid for compensation (Fig. 2). In our study, electricity prices are governed by a TOU pricing scheme containing three different electricity rates each day: peak load, mid-load, and off-peak load, depending on the time of day. We consider two major decisions simultaneously: (1) assigning jobs to machines and determining machine statuses in each time period $t \in T$ to minimize total weighted completion time (TWCT) and (2) determining energy transactions between the main grid, the manufacturing plant, and operating ESSs to minimize energy cost (EC).

3.1. Model

Apart form what has already been stated, we further make the following assumptions for our problem:

1. All machines and jobs are available at the beginning of our time horizon T;
2. All jobs are required to be processed completely by the end of the time horizon T;
3. The processing order of jobs can differ among flowshop stages;
4. Each machine can process only one job at a time;

5. Each machine must complete job j before undergoing a setup or processing another job $j' \in J \setminus \{j\}$;

Using the above notation, the objective function and constraints of the proposed MILP model for flow shop scheduling and energy supply decisions are given as follows:

$$\min \text{TWCT} = \sum_{j\in J} w_j \sum_{t\in T}(tl + p_{|M|j} - l)x_{|M|jt} \tag{1}$$

$$\min \text{EC} = \sum_{t\in T}(c_t^d d_t l + \sum_{i\in B} c_{it}^E E_{it} - c_t^u u_t \rho_t l) \tag{2}$$

Subject to

$$y_{m-1,jt} + y_{mjt} \le 1 \qquad \forall m \in M \setminus \{1\}, j \in J, t \in T, \tag{3}$$

$$\sum_{\tau=1}^{t} x_{m-1,j\tau} \ge \sum_{\tau=1}^{t} x_{mj\tau} \qquad \forall m \in M \setminus \{1\}, j \in J, t \in T, \tag{4}$$

$$\sum_{\tau\ge 1}^{\tau\le |T|-\frac{p_{mj}}{l}+1} x_{mjt} = 1 \qquad \forall m \in M, j \in J, \tag{5}$$

$$y_{mjt} + \sum_{k\in J\setminus\{j\}} x_{mkt} \le 1 \qquad \forall m \in M, j \in J, t \in T \tag{6}$$

$$l \sum_{\tau\ge t}^{\tau\le t+\frac{p_{mj}}{l}-1} y_{mj\tau} \ge x_{mjt} \cdot p_{mj} \qquad \forall m \in M, j \in J, t \in \{1, 2, \ldots, |T| - \frac{p_{mj}}{l} + 1\}, \tag{7}$$

$$l \sum_{\tau\ge t}^{\tau\le t+\frac{s_{fg}}{l}-1} o_{mfg\tau} \ge v_{mfgt} \cdot s_{fg} \qquad \forall m \in M, f \in F, g \in F \setminus \{g\}, t \in T, \tag{8}$$

$$\sum_{j\in J} y_{mjt} + \sum_{f\in F} z_{mft} + \sum_{k\in F}\sum_{h\in F\setminus\{k\}}\sum_{\tau>t-\frac{s_{kh}}{l}}^{\tau\le t} v_{mkh\tau} = 1 \qquad \forall m \in M, t \in T, \tag{9}$$

$$z_{mft-1} + \sum_{F_j=f} y_{mj,t-1} + \sum_{g\in F\setminus\{f\}} v_{mgf,t-\frac{s_{gf}}{l}} = z_{mft} + \sum_{F_j=f} y_{mjt} + \sum_{g\in F\setminus\{f\}} v_{mfgt} \qquad \forall m \in M, f \in F, t \in T \setminus \{1\}. \tag{10}$$

$$d_t - u_t\rho_t - \sum_{i\in B} b_{it} - a_t = \sum_{m\in M}\sum_{j\in J} y_{mjt} q_{mj}^y + \sum_{m\in M}\sum_{f\in F} z_{mft} q_{mf}^z + \sum_{m\in M}\sum_{f,g\in F: f\ne g} o_{mfgt} q_{mfg}^l - \sum_{r\in R} \tilde{\omega}_{rt} \qquad \forall t \in T, \tag{11}$$

$$b_i^{min} \le b_{it} \le b_i^{max} \qquad \forall i \in B, t \in T, \tag{12}$$

$$E_{it} = E_{i,t-1} + b_{it} l \qquad \forall i \in B, t \in T, \tag{13}$$

$$E_{it}^{min} \le E_{it} \le E_{it}^{max} \qquad \forall i \in B, t \in T, \tag{14}$$

$$u_t l \le \sum_{r\in R} r_{rt} \qquad \forall t \in T, \tag{15}$$

$$x_{mjt}, y_{mjt}, z_{mft}, o_{mfgt}, v_{mfgt} \in \{0, 1\} \qquad \forall m \in M, j \in J, f, g \in F, t \in T, \tag{16}$$

$$d_t, u_t, E_{it}, a_t \ge 0 \qquad \forall i \in B, t \in T, \tag{17}$$

b_{it} unrestricted $\qquad \forall i \in B, t \in T.$ (18)

Eqs. (1) and (2) define the two objective functions that our model seeks to simultaneously minimize: (1) total weighted completion time and (2) energy costs, which we calculate as the cost of purchasing power from the grid plus the cost of storing energy in ESSs, minus the revenue generated from selling power back to the grid. Constraint set (3) ensures that job j can only be processed by one machine during any time period $t \in T$. Next, constraint set (4) guarantees that any job j must be processed on machine $(m-1)$ before it can be processed on machine m due to the flow shop environment under study. Constraint set (5) requires that any job j can only be processed by each machine m once. Next, constraint set (6) ensures that any machine m can process job j only after job j is assigned to the machine. Any machine m cannot be interrupted once it starts processing a job, which is guaranteed by constraint set (7). Similarly, constraint set (8) ensures that a setup operation on machine m cannot be interrupted once it starts.

The constraints for representing the three machine states of interest are inspired by Sourd (2005). Constraint set (9) ensures that any machine can only be in exactly one state, job processing, setup, or idling, in each time period $t \in T$. Further, any change of machine state induces a setup operation (10). The power needed for running the flow shop's machines includes power purchased from the grid, power discharged from ESSs, and power generated by on-site renewable generators. Constraint set (11) is a power balance equation which specifies that the total available power should meet the total power demand at every time period. In (11), b_{it} is the charging/discharging rate of ESS $i \in B$ during time period $t \in T$. The value of b_{it} will be positive if the ESS $i \in B$ is charging; otherwise, it is in a discharging mode. These decisions are bounded by the charging/discharging rates of the ESS (12). Constraint set (13) is the system dynamics equations which specify the state of ESS $i \in B$ (see Wang, Gangammanavar et al. (2019) for details). In (13), the initial state E_{i0} is assumed to be given. Constraint set (14) ensures that the state of ESS $i \in B$ is always between its lower and upper bounds. The quantity of renewable generation determines the upper bound of the power sold to the main grid (15). Finally, constraint sets (16)–(18) provide variable types and limits on the decision variables in our model.

3.2. Formulation of the two-stage stochastic programming model

The proposed scheduling and energy supply problem can be written as a two-stage stochastic program (2-SP) to model the stochastic nature of on-site renewable energy resources. Since scheduling decisions are made prior to the realization of renewable energy availability, they are non-anticipative in nature (Birge & Louveaux, 2011). We succinctly use a single decision vector $x \in \mathcal{X}$ to collectively denote scheduling variables x_{mjt}, y_{mjt}, z_{mft}, o_{mfgt} and v_{mfgt}, where $\mathcal{X}$ denotes the feasible set. Once scheduling decisions are made, energy supply requirements are informed by this decision vector and the realization of renewable generation ω of its stochastic process $\tilde{\omega}$. This allows us to write the entire model as:

$$\min \sum_{j\in J} w_j \sum_{t\in T}(tl + p_{|M|j} - l)x_{|M|jt} + \mathbb{E}\{h(x, \omega)\} \tag{19a}$$

s.t. (3.3) – (3.10) and (3.16),

where the recourse function $h(x, \omega)$ is given by:

$$h(x, \omega) = \min \sum_{t\in T}(c_t^d d_t - c_t^u u_t + \sum_{i\in B} c_{it}^E E_{it}) \tag{19b}$$

s.t. (3.11) – (3.15), (3.17), and (3.18).

According to the general formulation of a stochastic problem (Birge & Louveaux, 2011), problem (19a) is commonly referred to as the master problem, while problem (19b) is known as the subproblem. Note that the decision variables in the master problem (19a) are binary variables, while the decision variables in subproblem (19b) are continuous. While first-stage decisions affect the right-hand side of Eq. (11) (renewable generation), the recourse matrix characterized by the left-hand side in Eq. (11) and the transfer matrix characterized by the right-hand side of Eq. (11) are independent of uncertainty. Therefore, the above formulation is a 2-SP with fixed recourse (Birge & Louveaux, 2011).

4. Two-stage, multi-objective stochastic solution scheme

Our problem is a bi-objective problem whose solution is described by a Pareto-optimal set, rather than a unique solution. In general, the resolution of multi-objective stochastic problems involves two kinds of transformations: transforming the multi-objective problem into a single-objective problem and converting the stochastic problem into its equivalent deterministic problem (Abdelaziz et al., 1999; Stancu-Minasian, 1984). Caballero et al. (2004) classify the existing techniques for the solution of multi-objective stochastic problems according to

the order in which transformations are carried out. The *multi-objective* approach first transforms the stochastic multi-objective problem into its equivalent multi-objective, deterministic problem. Alternatively, the *stochastic* approach transforms the stochastic multi-objective problem into a single-objective stochastic problem in the first step.

Multi-objective stochastic optimization approaches have been studied in various fields. Tricoire et al. (2012) formulate a bi-objective stochastic covering tour problem using a sample average approximation (SAA) technique, which is then solved by a branch-and-cut method within an ϵ-constraint algorithm. Osorio et al. (2018) provide an approach which combines the SAA method and the augmented ϵ-constraint algorithm. Biel et al. (2018) propose a two-stage stochastic optimization framework for flow shop scheduling problems with on-site wind power. In the first stage, a bi-objective MILP is formulated via an ESF considering all generated wind power scenarios simultaneously. The bi-objective objective function is transformed into a single objective using a weighted sum approach. In the second stage, energy supply decisions are adjusted according to the realization of actual wind power. Compared to the ϵ-constraint algorithm, weighted sum approach has two main drawbacks (Tricoire et al., 2012): (1) it is difficult for decision-makers to define weights for conflicting objectives a priori; and (2) it can only find supported solutions and missing other attractive candidates. So motivated by Cardona-Valdés et al. (2011), our solution approach for solving the bi-objective stochastic problem adopts an ϵ-constraint framework to transform the multi-objective problem into a problem with only one objective. The L-shaped method is used to tackle the 2-SP. The details of ϵ-constraint framework and the L-shaped method described in the following subsections.

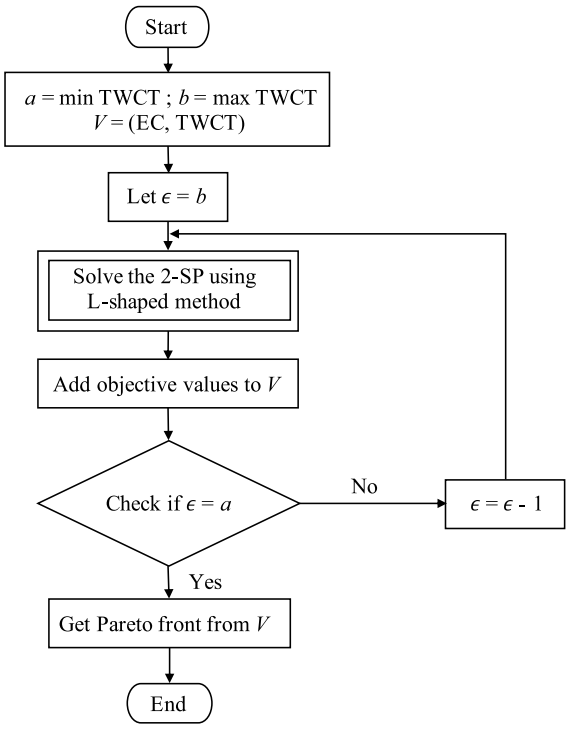

Fig. 3. Flowchart of two-stage multi-objective stochastic solution scheme (Cardona-Valdés et al., 2011).

4.1. ϵ-constraint framework

The ϵ-constraint algorithm (Haimes, 1971) consists of transforming a multi-objective problem into a single objective problem. To do this, decision-makers must select one objective function to remain as the objective function and transform all others into constraints bounded by a set of parameters ϵ. These additional constraints are named as ϵ-constraints.

To enumerate all Pareto optimal solutions, the algorithm iteratively solves single-objective optimization problems for each value of the ϵ parameters. The formulation introduced in Section 3 has two objective functions: TWCT and EC. The discrete-time periods result in integer values of TWCT. If we convert TWCT into an ϵ-constraint, it is easy to change the value of parameter ϵ by one unit from one iteration to the next (Cardona-Valdés et al., 2011). Therefore, for computational convenience, we choose EC as the main objective function and TWCT is transformed into an ϵ-constraint. By introducing these changes, the master problem (19a) can be reformulated as:

$$\min \mathbb{E}\{h(x,\omega)\} \tag{20}$$
$$\text{s.t.} \sum_{j\in J} w_j \sum_{t\in T}(tl + p_{|M|j} - l)x_{|M|jt} \le \epsilon$$
$$(3.3) - (3.10),\ (3.16).$$

Note that the two-stage stochastic programming framework in problem (20) is maintained by converting TWCT to an ϵ-constraint.

Fig. 3 shows a flow chart for the two decomposition algorithms integrated with the ϵ-constraint framework (Cardona-Valdés et al., 2011). Given the negative correlation between our two objective functions (i.e., TWCT increases as EC decreases), the maximum (minimum) value of TWCT, which is denoted as b (a), is obtained when EC reaches its smallest (largest) value. Let V denote a set of paired objective functions EC and TWCT. We begin our algorithm by setting the value of parameter $\epsilon = b$. The ϵ value is decreased by one unit (δ) in each iteration. We call this an ϵ-iteration within which one pair of optimal solutions is obtained using our decomposition algorithms. Note that ϵ is an upper bound of TWCT, not the value of TWCT. The actual TWCT value can be calculated using the ϵ-constraint during each ϵ-iteration. The ϵ-iteration stops when $\epsilon = a$. Finally, the Pareto front is identified from the set V.

4.2. L-shaped method

Classical 2-SPs are well studied in the literature and several algorithms have been proposed to analyze these problems. To achieve computational tractability, many of these methods represent uncertainty through a finite number of realizations (scenarios). The expected value of the second stage function is computed by taking the average of M individual objective values obtained from each scenario. The expectation function can be replaced by its SAA and re-stated as follows (Kleywegt et al., 2002):

$$H(x) = \frac{1}{M}\sum_{i=1}^{M} h(x,\omega^i). \tag{21}$$

Decomposition-based methods, such as Dantzig–Wolfe decomposition (Dantzig & Wolfe, 1960), progressive hedging (Rockafellar & Wets, 1991), and L-shaped method (Van Slyke & Wets, 1969), have proven effective in solving the SAA. These methods iteratively build piecewise affine approximations to the expected recourse function by solving a subproblem for each scenario from a set of scenarios. Dantzig–Wolfe decomposition is not directly applicable for MILP problems as it solves the dual of the master problem. Progressive hedging, which is a scenario-based decomposition method, requires selecting an appropriate proximal parameter which is instance-dependent and hard to determine. We base our solution approach on the L-shaped method.

To simplify our exposition of L-shaped method, we use a succinct representation of the 2-SP model (Birge & Louveaux, 2011):

$$\min c^\top x + \mathbb{E}\{h(x,\omega)\} \tag{22a}$$
$$\text{s.t. } x \subset \mathbb{Z}^{n_1} \times \mathbb{R}^{n_2},$$

Table 2
Input ϵ, corresponding TWCT, and predicted EC of Ins3s.

ϵ	TWCT (h)	Predicted EC ($)	ϵ	TWCT (h)	Predicted EC ($)	ϵ	TWCT (h)	Predicted EC ($)
138[a]	135	233.737	130	129	240.391	122	120	253.878
137	135	234.104	129[a]	129	240.391	121	120	253.878
136	135	234.104	128	126	245.790	120[a]	120	253.878
135	135	234.104	127	126	245.790	119	117	257.558
134	132	234.988	126[a]	126	245.790	118	117	257.558
133	132	234.988	125	123	250.909	117[a]	117	257.558
132[a]	132	234.988	124	123	250.909			
131	129	240.391	123[a]	123	250.909			

[a]Pareto optimal solution.

where

$$h(x,\omega) = \min\ d^{\top}y \tag{22b}$$
$$s.t.\ Wy \le r(\omega_n) - T(\omega)x,$$
$$y \ge 0.$$

Auxiliary variable η is used to represent the approximation of the expected recourse function $\mathbb{E}\{h(x,\omega)\}$. At the beginning of the algorithm, the value of η is set as $-\infty$ or an appropriate approximation value. The algorithm begins with the original constraints only, $\mathcal{X}^0 := \{x,\eta | Ax = b\} \subset \mathbb{Z}_+ \times \mathbb{R}_+$. In iteration k, the algorithm first solves the MILP

$$\min\{c^{\top}x + \eta | (x,\eta) \in \mathcal{X}^k\}, \tag{23}$$

to obtain the solution x^k. Then, with this solution and a realization $\omega_i \in \Omega$, the optimal dual solution π^k is identified by solving the subproblem $h(x^k,\omega_i)$. This procedure is enumerated for every realization $\omega_i \in \Omega$. Using these dual solutions, we obtain a lower bounding optimality cut as follows:

$$l^k(x,\eta) := \sum_{i\in S} p_i \pi_i^{\top}[r(\omega^i - T(\omega^i)x^k)] - \eta \le 0, \tag{24}$$

where p_i is the probability of scenario ω_i and S is the number of scenarios. Then, the feasible region is updated as:

$$\mathcal{X}^{k+1}(x) = \mathcal{X}^k(x) \cap (l^k(x,\eta) \le 0). \tag{25}$$

Note that our subproblem (19b) satisfies the relative complete recourse property which means our subproblem has feasible solutions for all $\omega_i \in \Omega$ and $x \in \mathcal{X}^0$. Therefore, we omit feasibility cuts here. For more details, we refer the reader to Birge and Louveaux (2011).

5. Computational experiments

We consider a three-machine flow shop in which three jobs need to be processed within the planning horizon (T = 24 h). The length of each time slot is one hour and 10 random problem instances are created. The data for weights of the jobs (w_j), job processing times (p_{mj}), and the processing power requirements of machines (q^y_{mj}) are from Biel et al. (2018). Setup times (s_{fg}) and the power consumed during setup (q^l_{mfg}) are randomly generated from uniform distributions [1 h, 3 h] and [1 kW, 15 kW], respectively.

One energy storage system is installed and available near the plant. Renewable generation data was extracted from the Western Wind and Solar Integration Study (NREL, 2016). An experiment utilizes solar generation if no specific details are given. To reduce the impact of seasonal variations, we only adopt the renewable generation data from spring. The number of scenarios considered in building our instances is 1000. Electricity prices follow a day-ahead TOU pricing scheme (Fig. 4) which is derived from a rate schedule for industrial customers of California's Pacific Gas and Electric Company (Pacific Gas and Electric Company, 2018a). The feed-in electricity price is set to 0.08923 USD/kWh as found in the Electric-Renewable Market Adjusting Tariff of the Pacific Gas and Electric Company (Pacific Gas and Electric Company, 2018b).

Our L-shaped method-based ϵ-constraint algorithm was implemented in C on a MacBook Pro running an Intel Core i7 CPU@3.3 GHz (Dual-Core) with 16 GB Memory @2133 MHz. All MILPs were solved using CPLEX 12.7 callable subroutines.

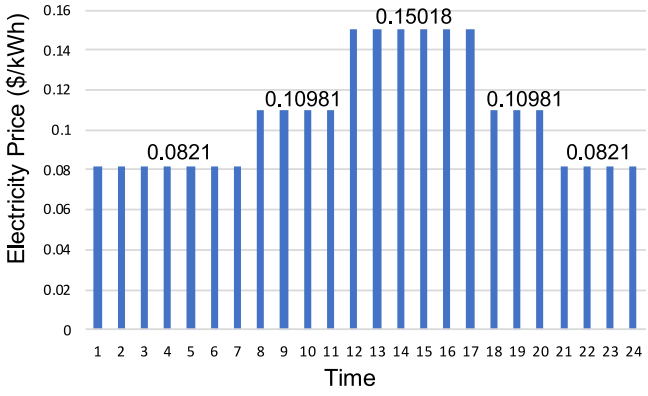

Fig. 4. TOU pricing scheme.

During each ϵ-iteration, we begin by using an optimization process to identify the optimal solution for the master problem and the corresponding prediction value. Then, a verification phase is applied, where the solution of the master problem is fixed, and the subproblem is simulated using independent and identically distributed observations. Using the objective values, a confidence interval (CI) of the upper bound estimate is built for the expected recourse function.

We begin by illustrating how the ϵ-constraint framework works using instance 3 ("Ins3s"). The input ϵ value, corresponding TWCT, and predicted EC are summarized in Table 2. As mentioned in Section 4.1, the actual TWCT is not necessarily equal to the input ϵ, which is shown in the results in the 2nd, 5th, and 8th columns in Table 2. For example, when ϵ is equal to 138, the actual TWCT is 135. Another feature that should be noted is that TWCT is 135 whenever the input ϵ is set to 138 or 135. The predicted EC obtained when ϵ is set to 138 is smaller than the value obtained when ϵ is changed to 135. Therefore, (TWCT = 138, EC = 233.737) is Pareto optimal as (TWCT = 138, EC = 233.737) dominates (TWCT = 135, EC = 234.104), although this Pareto point is obtained when the input ϵ is 138 not 135. We say a point (TWCT, EC) dominates another point (TWCT′, EC′) when TWCT′ ≥ TWCT and EC ≤ EC′. Therefore, seven Pareto optimal solutions are found for instance 3, marked by "*" in Table 2. Fig. 5 presents the Pareto frontier of the ten instances. As we expected, there is a trade-off between TWCT and the predicted objective value EC: as the TWCT decreases, the predicted EC increases.

Next, we continue to use instance 3 to study the effect of setup costs in our scheduling problem with both time and energy cost considerations. We create another problem using Ins3s without considering setup costs, Ins3. Ins3 also contains seven Pareto optimal solutions which obtain the same TWCT as Ins3s. Fig. 6 presents the differences in energy costs between these two problem instances. We see that the differences consistently fall in the range [2.85%, 3.2%] for each

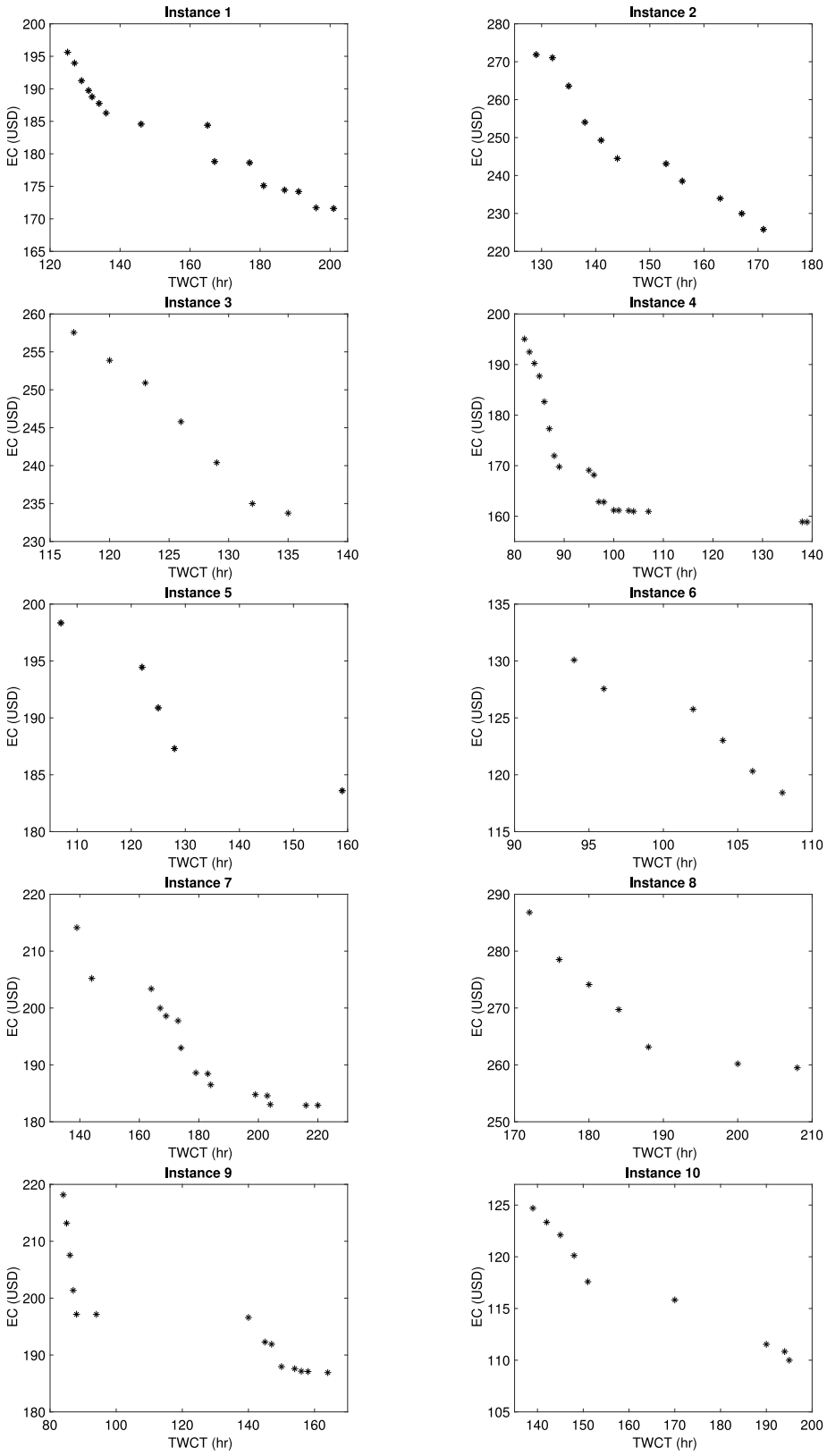

Fig. 5. Pareto fronts of all 10 instances.

TWCT. The average difference value is 2.94%, while the average power requirement for setup operations is approximately 6.5% of the power required by job processing. This analysis confirms for decision-makers that the energy costs of setup operations cannot be ignored, especially for some industries in which setup operations consume a large amount of energy.

Next, we study the impact of integrating on-site renewable energy and different sources of renewable energy on the production schedules

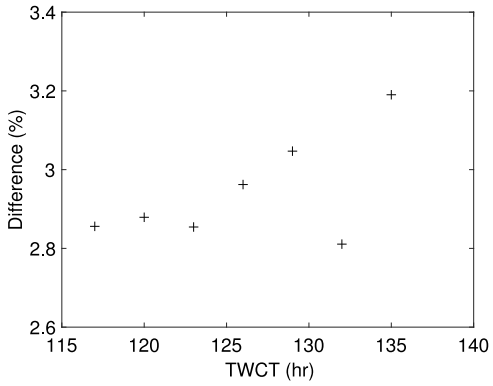

Fig. 6. Cost differences between instance Ins3s and Ins3.

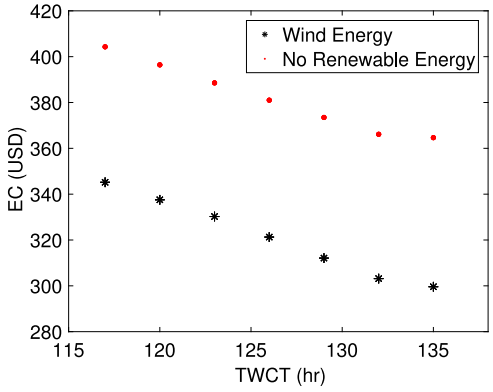

Fig. 7. Pareto front for instance 3 with wind energy and without renewable energy.

and energy costs for problem Ins3s. Two more instances are created—one with wind energy as the renewable energy source and the other instance has no renewable energy at all. Wind and solar penetrations are kept the same in the first two instances. In the no-renewable instance, the random variable $\tilde{\omega}_{rt}$ is set to 0 for all generators at every time period. To this end, the studied bi-objective stochastic model is turned into a bi-objective deterministic program. Fig. 7 shows the Pareto frontier of the studied example problems with wind energy and without renewable energy. Both of these two instances found seven Pareto optimal solutions at the same TWCT as Ins3s did. All three instances have the same trend of reducing EC when increasing TWCT.

During the verification phase, 100 samples are used for different ϵ parameters to evaluate the solution. Fig. 8 presents the energy costs observed at every TWCT of all three problem instances during the verification phase. It clearly shows that incorporating renewable energy helps to reduce energy costs for production. On average, using solar energy and wind energy saves 35.8% and 15.9% over no renewable generation utilized, respectively. Another observation from Fig. 8 is that cost reduction is more prominent when utilizing solar energy than with wind energy as the average savings is 23.6%. This decrease can be attributed to the different distributions of solar and wind generation within the time horizon of interest (Fig. 9). Wind power distributes evenly during the entire time horizon (Fig. 9(b)), while solar provides more generation during the day time when electricity prices are high (Fig. 4). Therefore, solar energy can satisfy some or all power demand during these high electricity price periods. Moreover, surplus solar energy can be stored in energy storage devices for future use or fed back into the main grid for compensation.

To further study the impact of on-site renewable energy on production schedules and energy costs, we use the optimal first-stage solution as an input to the subproblem. The decision process of the subproblem is simulated by solving an optimization problem using independent Monte Carlo samples. Fig. 10 shows the results with and without solar energy when TWCT = 132. Production processes, which consume more energy, are scheduled within low-electricity-price periods as much as possible to save energy costs in both of these two cases. With the help of renewable on-site renewable energy, production and setups can be performed in time periods within with higher electricity prices. For example, the start of job 2's processing on machine 2 is scheduled four time slots earlier when solar energy is available than in the schedule when no renewable energy is available. Another example is that the setup operation of changing family 1 to family 2 on machine 3 is moved from time window (Kleywegt et al., 2002; Liu, 2016) to (Fazli Khalaf & Wang, 2018; Gahm et al., 2016) to fully utilize renewable energy. Fig. 10 also shows that during time periods (Ding et al., 2016; Haimes, 1971), renewable energy not only satisfies production requirements but also is sold back to the grid for compensation. Another interesting observation from Fig. 10 is that the storage device is charged during time periods 7 and 11, the last periods before the electricity prices increase, regardless of whether renewable energy is used or not. The stored energy then is released to the system for production in future high electricity price time periods. These charging and discharging activities help to reduce total energy costs. The energy device only stores energy for one time period after each charging activity as the trade-off between storage cost and power purchasing cost determines the length of storage periods.

6. Conclusions and future research

In this paper, we study a flow shop scheduling problem with sequence-dependent setups, on-site renewable generation, and an available energy storage system. The model is formulated as a two-stage, multi-objective stochastic MILP. In the first stage, a time-indexed MILP is proposed to capture sequence-dependent setups. The optimal production schedule is determined to minimize the total weighted completion time. The second stage determines the energy supply decisions according to the production schedule and the realization of renewable energy generation to minimize energy costs under a TOU electricity price scheme. To solve this problem, we first adopt a ϵ-constraint approach to transform the multi-objective problem into a two-stage, single-objective stochastic MILP which is then tackled by Benders' decomposition.

Experiments based on machine power requirements, real renewable generation, a current TOU tariff, and a renewable feed-in tariff produce sets of Pareto optimal solutions for decision-makers who want to minimize total weighted completion time and energy cost in scheduling production process. Among sets of Pareto optimal solutions, decision-makers can choose the Pareto solution according to their preferences to determine job processing sequence and operate on-site ESSs. Sensitivity analysis shows that the energy cost of setup operations is relatively high compared to the power requirements of setup operations such that they cannot be ignored. Our experiments also reveal that both solar generation and wind generation are capable of reducing energy costs. However, energy cost reductions are more prominent by using solar energy than by using wind energy. This is because solar and wind generation follow different distributions during the time horizon under study. Finally, we studied how production schedules and energy supply change with the utilization of solar energy during the day.

The obtained results are associated with the available data of specific region and season. Further, we do not differentiate the electricity prices between working days and weekends. The number of working hours in one day is assumed as 24 h in our numerical example that maybe not the usual schedule of some manufacturing factories. However, our developed methodology can be applied and customized to any given data including the electricity prices and renewable generation data in other regions/seasons, and any number of working hours in a workday. From the case study, several managerial implications can be derived: (1) Our model can be used as a managerial tool to

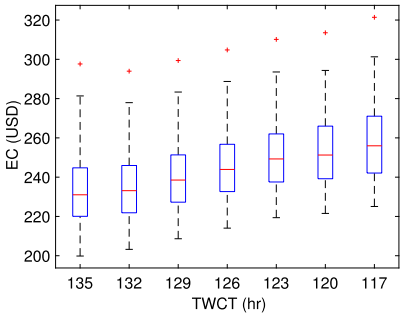

(a) Objective values of instance 3 with solar energy

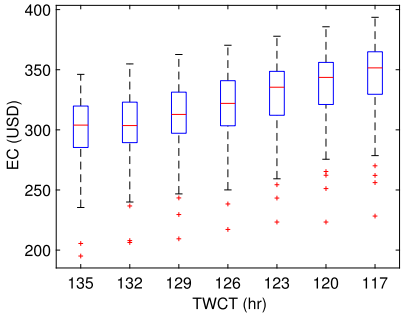

(b) Objective values of instance 3 with wind energy

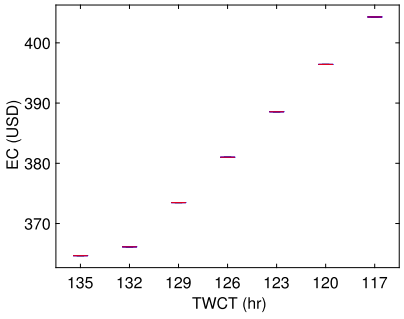

(c) Objective values of instance 3 without renewable energy

Fig. 8. Objective values of instance 3.

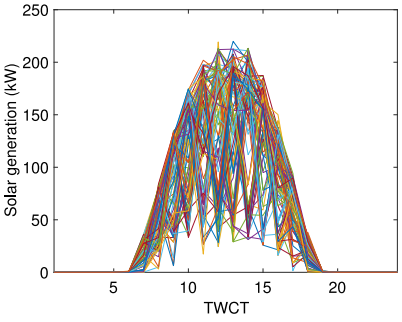

(a) Distribution of solar generation

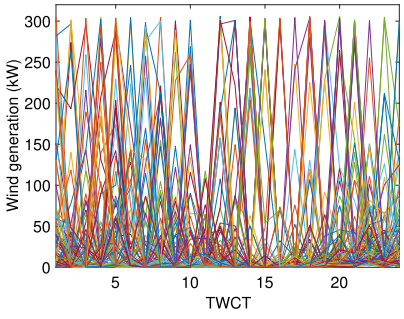

(b) Distribution of wind generation

Fig. 9. Distributions of solar and wind generation.

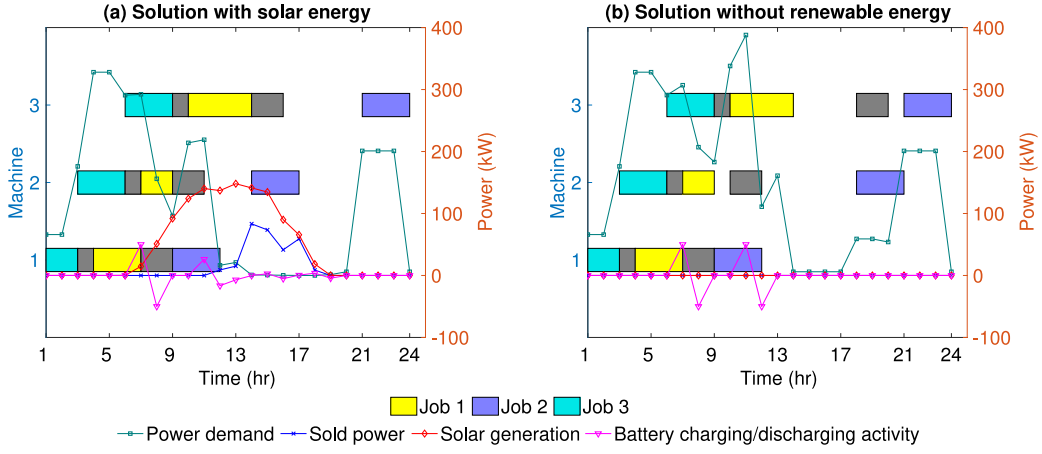

Fig. 10. Comparison of production schedules of instance 3 with and without solar energy.

optimize production scheduling and energy cost simultaneously with regards to one day-ahead TOU electricity pricing scheme and stochastic renewable generation; (2) manufacturing factories need to consider scheduling setups while optimizing time-dependent energy cost; (3) renewable generation resources, especially the solar panel, play a crucial role in reducing energy cost and promoting environmental goals in manufacturing.

There are several potential extensions for our study. First, we worked with small flow shop instances for computational efficiency. To address large-scale problems effectively, future research should focus on developing heuristic/meta-heuristic algorithms for this challenging problem. Another area for further research is to consider other machine environments such as job shops, which are prevalent in practice. Further, investigating production schedules and energy supply decisions under hour-ahead real-time tariffs would introduce additional uncertainty to the problem for another interesting line of research.

CRediT authorship contribution statement

Shasha Wang: Conceptualization, Methodology, Software, Validation, Investigation, Writing - original draft. **Scott J. Mason:** Conceptualization, Methodology, Investigation, Supervision, Writing - review & editing. **Harsha Gangammanavar:** Methodology, Resources, Writing - review & editing.

References

Abdelaziz, F., Lang, P., & Nadeau, R. (1999). Dominance and efficiency in multicriteria decision under uncertainty. *Theory and Decision*, *47*(3), 191–211.

Allahverdi, A., & Soroush, H. (2008). The significance of reducing setup times/setup costs. *European Journal of Operational Research*, *187*(3), 978–984.

Biel, K., & Glock, C. H. (2016). Systematic literature review of decision support models for energy-efficient production planning. *Computers & Industrial Engineering*, *101*, 243–259.

Biel, K., Zhao, F., Sutherland, J. W., & Glock, C. H. (2018). Flow shop scheduling with grid-integrated onsite wind power using stochastic milp. *International Journal of Productions Research*, *56*(5), 2076–2098.

Birge, J. R., & Louveaux, F. (2011). *Introduction to stochastic programming*. Springer Science & Business Media.

Caballero, R., Cerdá, E., del Mar Muñoz, M., & Rey, L. (2004). Stochastic approach versus multiobjective approach for obtaining efficient solutions in stochastic multiobjective programming problems. *European Journal of Operational Research*, *158*(3), 633–648.

Cardona-Valdés, Y., Álvarez, A., & Ozdemir, D. (2011). A bi-objective supply chain design problem with uncertainty. *Transportation Research Part C: Emerging Technologies*, *19*(5), 821–832.

Dantzig, G. B., & Wolfe, P. (1960). Decomposition principle for linear programs. *Operations Research*, *8*(1), 101–111.

Ding, J. Y., Song, S., Zhang, R., Chiong, R., & Wu, C. (2016). Parallel machine scheduling under time-of-use electricity prices: New models and optimization approaches. *IEEE Transactions on Automation Science and Engineering*, *13*(2), 1138–1154.

Energy Information Adiministration (2017). International energy outlook 2017. URL: https://www.eia.gov/outlooks/ieo/pdf/0484(2017).pdf (Accessed: 2019-1-28).

Energy Information Adiministration (2020a). Use of energy explained. URL: https://www.eia.gov/energyexplained/use-of-energy/industry.php (Accessed: 2020-1-5).

Energy Information Adiministration (2020b). EIA Monthly energy review. URL: https://www.eia.gov/totalenergy/data/monthly/pdf/mer.pdf (Accessed: 2020-1-5).

Eric, L., Benjamin, S., Michael, G., Robert, P., & Ian, B. G. (2016). Assessing the future of distributed wind: Opportunities for behind-the-meter projects. URL: https://www.nrel.gov/docs/fy17osti/67337.pdf (Accessed: 2018-1-12).

Fazli Khalaf, A., & Wang, Y. (2018). Energy-cost-aware flow shop scheduling considering intermittent renewables, energy storage, and real-time electricity pricing. *International Journal of Energy Research*, *42*(12), 3928–3942.

Gahm, C., Denz, F., Dirr, M., & Tuma, A. (2016). Energy-efficient scheduling in manufacturing companies: a review and research framework. *European Journal of Operational Research*, *248*(3), 744–757.

Giret, A., Trentesaux, D., & Prabhu, V. (2015). Sustainability in manufacturing operations scheduling: A state of the art review. *Journal of Manufacturing Systems*, *37*, 126–140.

Haimes, Y. (1971). On a bicriterion formulation of the problems of integrated system identification and system optimization. *IEEE Transactions on Systems, Man, and Cybernetics*, *1*(3), 296–297.

Kleywegt, A. J., Shapiro, A., & Homem-de Mello, T. (2002). The sample average approximation method for stochastic discrete optimization. *SIAM Journal on Optimization*, *12*(2), 479–502.

Liu, C. H. (2016). Mathematical programming formulations for single-machine scheduling problems while considering renewable energy uncertainty. *International Journal of Productions Research*, *54*(4), 1122–1133.

Liu, G. S., Zhou, Y., & Yang, H. D. (2017). Minimizing energy consumption and tardiness penalty for fuzzy flow shop scheduling with state-dependent setup time. *Journal of Cleaner Production*, *147*, 470–484.

Luo, H., Du, B., Huang, G. Q., Chen, H., & Li, X. (2013). Hybrid flow shop scheduling considering machine electricity consumption cost. *International Journal of Production Economics*, *146*(2), 423–439.

Moon, J. Y., & Park, J. (2014). Smart production scheduling with time-dependent and machine-dependent electricity cost by considering distributed energy resources and energy storage. *International Journal of Productions Research*, *52*(13), 3922–3939.

NREL (2016). Solar power data for integration studies. URL: https://www.nrel.gov/grid/solar-power-data.html (Accessed: 2019-1-28).

Osorio, A. F., Brailsford, S. C., & Smith, H. K. (2018). Whole blood or apheresis donations? A multi-objective stochastic optimization approach. *European Journal of Operational Research*, *266*(1), 193–204.

Pacific Gas and Electric Company (2018a). Industrial/general service (e-20). https://www.pge.com/tariffs/electric.shtml#INDUSTRIAL (Accessed: 2018-12-23).

Pacific Gas and Electric Company (2018b). Remat feed-in tariff (senate bill 32). URL: https://www.pge.com/en_US/for-our-business-partners/floating-pages/remat-feed-in-tariff/remat-feed-in-tariff.page (Accessed: 2018-12-23).

Rockafellar, R., & Wets, R. J.-B. (1991). Scenarios and policy aggregation in optimization under uncertainty. *Mathematics of Operations Research*, *16*(1), 119–147.

Sharma, A., Zhao, F., & Sutherland, J. W. (2015). Econological scheduling of a manufacturing enterprise operating under a time-of-use electricity tariff. *Journal of Cleaner Production*, *108*, 256–270.

Sourd, F. (2005). Earliness–tardiness scheduling with setup considerations. *Computers & Operations Research*, *32*(7), 1849–1865.

Stancu-Minasian, I. M. (1984). *Stochastic programming with multiple objective functions, Vol. 13*. D Reidel Pub Co.

Tricoire, F., Graf, A., & Gutjahr, W. J. (2012). The bi-objective stochastic covering tour problem. *Computers & Operations Research*, *39*(7), 1582–1592.

Van Slyke, R. M., & Wets, R. (1969). L-shaped linear programs with applications to optimal control and stochastic programming. *SIAM Journal of Applied Mathematics*, *17*(4), 638–663.

Wang, S., Gangammanavar, H., Ekşioğlu, S. D., & Mason, S. J. (2019). Stochastic optimization for energy management in power systems with multiple microgrids. *IEEE Transactions on Smart Grid*, *10*(1), 1068–1079.

Wang, S., Kurz, M., Mason, S. J., & Rashidi, E. (2019). Two-stage hybrid flow shop batching and lot streaming with variable sublots and sequence-dependent setups. *International Journal of Productions Research*, 1–15.

Yildirim, M. B., & Mouzon, G. (2012). Single-machine sustainable production planning to minimize total energy consumption and total completion time using a multiple objective genetic algorithm. *IEEE Transactions on Engineering Management*, *59*(4), 585–597.

Zhai, Y., Biel, K., Zhao, F., & Sutherland, J. W. (2017). Dynamic scheduling of a flow shop with on-site wind generation for energy cost reduction under real time electricity pricing. *CIRP Annals*, *66*(1), 41–44.

Zhang, H., Cai, J., Fang, K., Zhao, F., & Sutherland, J. W. (2017). Operational optimization of a grid-connected factory with onsite photovoltaic and battery storage systems. *Applied Energy*, *205*, 1538–1547.